Archimedes screw generators for sustainable micro-hydropower production

Published as:

Simmons SC, Lubitz WD. Archimedes screw generators for sustainable micro-hydropower production. International Journal of Energy Research. 2021 Oct 10;45(12):17480-501.

SCOTT CHRISTOPHER SIMMONS, PhD. Candidate, *School of Engineering, University of Guelph, Guelph, Canada*

Email: ssimmons@uoguelph.ca

WILLIAM DAVID LUBITZ, Associate Professor, *School of Engineering, University of Guelph, Guelph, Canada*

Email: wlubitz@uoguelph.ca (author for correspondence)

Archimedes screw generators

Keywords

Archimedes screw generator, hydropower, Archimedes screw turbine, hydrodynamic screw, reverse Archimedes screw, run-of-river hydropower, renewable energy.

Abstract

Archimedes screws have been used as pumps since antiquity, and have more recently been implemented in micro-hydropower plants as an ecologically advantageous technology. They are regarded as a hydropower technology with lower environmental impact since they allow safe passage of aquatic flora and fauna through slow turning, widely spaced blades during operation. Archimedes screw generators operate at river-to-wire efficiencies at approximately 75% with relatively low installation and maintenance costs when compared to other hydropower technologies of the same scale. ASGs are relatively simple and cost efficient to manufacture – simple enough to create in the 7th century BCE. Modern manufacturing techniques for sheet metal and fabrication have refined ASG production. The literature contains various parametric models for predicting screw power output, and more recent numerical simulations have provided insight into the fluid mechanics of screw generators. The knowledge gained from these studies have allowed researchers to suggest more optimal designs for Archimedes screws. However, much can be done to further improve the accuracy of power prediction models. This paper discusses the current state of the literature for Archimedes screw generators, and highlights areas for future research to improve power prediction and optimization capabilities for researchers and industrial designers.

Keywords

Archimedes screw generator, hydropower, Archimedes screw turbine, hydrodynamic screw, reverse Archimedes screw, run-of-river hydropower, renewable energy.

Highlights

- Archimedes screws are an ancient pumping technology that have more recently found use as a hydropower-producing technology
- Archimedes screw generators (ASGs) are a small-scale hydropower technology that may be installed as a run-of-river installation

- ASGs are an eco-friendly technology that allow for the safe passage of sediments, small debris, fish, and other aquatic wildlife through their flights during operation.
- There are a few experiments and computational fluid dynamic (CFD) simulations that have sought to extend the literature's data on ASG operation.
- Current performance models for ASGs lack robust validation to be properly implemented in powerplant design.

Word Count

6804

Notation

A_w = wetted area of screw (m^2);
b_2 = inlet channel width (m);
C = hydraulic loss coefficient;
D_i = inner diameter (m);
D_o = outer diameter (m);
f = fill height ratio (-);
g = gravitational constant (9.81 m/s^2);
G_w = gap width (m);
ΔH = overall head (m);
h_1 = inlet model depth parameter (m);
h_2 = inlet model depth parameter (m);
h_G = geometric head (m);
h_L = lower water level (m);
h_L' = optimum lower water level (m);
h_U = upper water level (m);
L = flighted length (m);
l_e = gap leakage parameter (m);
l_w = gap leakage parameter (m);
n_b = number of buckets (-);
N = number of blades (-);
P_s = mechanical power at the screw's shaft (W);
$P_{L,f}$ = power loss due to friction (W);
$P_{L,OE}$ = power loss due to outlet expansion (W);
$P_{L,OS}$ = power loss due to outlet submergence (W);
Q = flow rate (m^3/s);
Q_b = bucket flow rate (m^3/s);
Q_g = gap leakage flow rate (m^3/s);
Q_o = overflow leakage rate (m^3/s);

R = outer radius (m)
S = screw pitch (m);
T = torque (Nm);
v_t = transport velocity (m/s);
V_b = bucket volume (m^3);
V_M = Muysken limit (m/s);
V_s = volume within screw's flights (m^3);
z_{min} = minimum bucket water level (m);
z_{max} = maximum bucket water level (m);
z_{wl} = bucket water level (m);
α = fluid phase, $\alpha = 1$ (water), $\alpha = 0$ (air);
β = inclination angle (°);
ζ_U = hydraulic loss factor (-);
ζ_L = Borda-Carnot exit loss coefficient (-);
η = efficiency (-);
μ = overflow leakage coefficient (-);
ρ = water density (998 kg/m^3);
Ψ_L = outlet submergence (-);
ω = screw rotation speed (rad/s); and
ω' = screw rotation speed (RPM);
ω_{nd} = non-dimensional screw rotation speed (-);

1. Introduction

The Archimedes screw (also called "hydrodynamic screw" or "Archimedean screw") has been utilized for various technological applications for over two millennia. An Archimedes screw consists of a helical array of blades wrapped around a central cylindrical tube. The screw is commonly inclined, fixed between upper and lower bearings, and enclosed in a concentric, open-topped trough. It may be operated as a pump, or as a hydroelectric generator (Figure 1). Volumes of water are trapped between the blades of the screw and the trough, forming what will hereafter be referred to as "buckets" [1]. Usually the trough is fixed, and the screw rotates within it. A small intentional gap exists between the blade tips and the trough to minimize friction and prevent blade and trough wear [2].

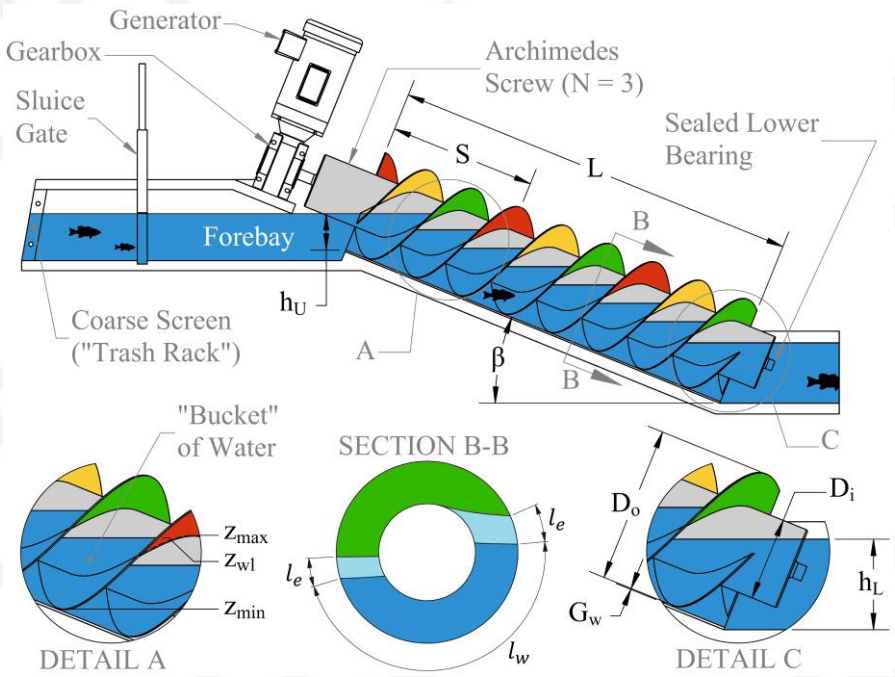

Figure 1: Archimedes screw generator layout and geometry. This figure will be referred to throughout the paper. Detail A presents the parameters often used when quantifying fill levels of screw "buckets". Section B illustrates the parameters used in gap leakage modelling techniques. Detail C demonstrates the outlet water level and gap width in higher resolution.

When implemented as a pump, mechanical power turns the screw, lifting water from a lower to upper reservoir as individual buckets form and translate upward along the screw. When implemented as a hydroelectric generator, water from an upper reservoir enters the top of the screw and causes a net rotation (turning a generator shaft) as it traverses the length of the screw and exits into a lower reservoir. At many low head, run-of-river hydropower sites, it may be advantageous to install an Archimedes screw generator (ASG) instead of a conventional hydropower turbine. ASGs are most appropriate at sites with low head and moderate flow rates [3]. Archimedes screws are theoretically reversible, and a few screw installations both pump and generate. At Stockton-on-Tees (UK) four parallel screws can pump water to supply high flow to an Olympic white water canoeing course, then operate as ASGs to produce electricity when canoe course flow is not required [4], [5].

2. Background

2.1. History

The Archimedes screw was used in antiquity as a pump for fluids and granular solids. Evidence suggests that the Archimedes screw may have been invented in Assyria in 7th century BCE under King Sennacherib (704-681 BCE) to water the gardens at the Assyrian capital of Nineveh; some scholars suggest that these were the Hanging Gardens of Babylon [6]. In 671 BCE, the Assyrian empire annexed Egypt [7] and likely introduced the technology for agricultural irrigation. Archimedes of Syracuse (the device's namesake, circa 287-212 BCE) studied in Alexandria where he might have learned of the technology and reintroduced, modified, reinvented or independently invented the device [1]. Archimedes popularized the device among his contemporaries by implementing it to irrigate the Nile delta [6], as the first recorded naval bilge pump [8], and purportedly in a ship for propulsion [9].

Archimedes screws were utilised during the Roman Imperial period (circa 27 BCE to circa 5th century CE), mainly to drain Roman mines [10] – after which its use is undocumented in the western world. It is suggested that mines in the Iberian Peninsula continued to use screw pumps during the Visigothic and Muslim regimes, and after the Reconquista [11]. The screw pumps in the mines of Aljustrel, Portugal [12] were maintained and improved during these periods. In 1637 CE, a crank-driven Archimedes screw was introduced in Japan, ostensibly by Portuguese traders [11]. Early Islamic literature evidences the continued use of screw pumps through the Middle Ages [10]. The *Maqamat al-Hariri* [13] is a famous collection of 50 poetic stories that were later illustrated by artists like Yahya ibn Mahmud al-Wasiti; one of his illustrations depicts a screw pump irrigating gardens [14].

The technology is much more prevalent in Renaissance literature [9]. It was documented by Konrad Kyser [15], Leonardo da Vinci [16], Gerolamo Cardano [17], Agostino Ramelli [18], and Galileo Galilei [19]. During the Dutch Golden Age (late 16th through 17th centuries) Archimedes screws were

implemented in polder mills [20] for land drainage and reclamation [21]. While originally powered by windmills, modern screw pumps use other means. For instance, UNESCO World Heritage site Kinderdijk (Netherlands) houses examples of its original 19 wind-powered polder mills; however, it is currently drained by two diesel-powered screw pumps and is one of the largest Archimedes screw pumping stations in Europe [22].

2.2. Modern Implementations

The robust, simple design of the Archimedes screw allows it to transport solids and fluids between its blades without obstruction – making it advantageous for a variety of implementations [23]. It has functioned as a water [24] and wastewater pump [25], a conveyor for granular solids (i.e. grains) [26], [27], a fish ladder [28]–[30], a drive mechanism for amphibious vehicles [31], for injection moulding [32], land reclamation [33], heart valve replacements [34], and for hydropower generation [35]. Note that this paper focuses on applications involving water conveyance.

Hydropower has been exploited since antiquity; however, no evidence suggests that Archimedes screws were implemented in functions other than pumping until the early 1900's [9]. A 1916 US patent suggested using an Archimedes screw to power a hydraulic system [36]. Kawakami [37] reports that small, transportable screw-mills were used as power sources in 1930's Japan before the introduction of engines and electric motors. The first instance of a screw operating as a hydro-electric generator is a 1991 patent [2] that describes a modern, inclined-axis, fixed-trough Archimedes screw generator; the most common implementation, since proven successful in hundreds of installations [38].

ASGs have an alternate, horizontal-axis orientation in which the screw is partially submerged in-stream at the free-surface, supported horizontally between bearings and oriented at an angle to the direction of flow, converting hydrokinetic energy to mechanical energy. Preliminary investigations have

demonstrated success, and Archimedes screws continue to be studied in this orientation [39], [40] however it has not been widely adopted. This review focuses on the inclined axis ASG variant.

3. Characteristics of Archimedes screw generators

3.1. Performance and power production capabilities

Figure 2 shows the performance envelope of different hydropower technologies. ASGs operate with low heads (< 6 m) and moderate flow rates (< 15 m^3/s) [41] at river-to-wire efficiencies of 60% to 80% [41], [42]; some installations reportedly operate at higher efficiencies [43].

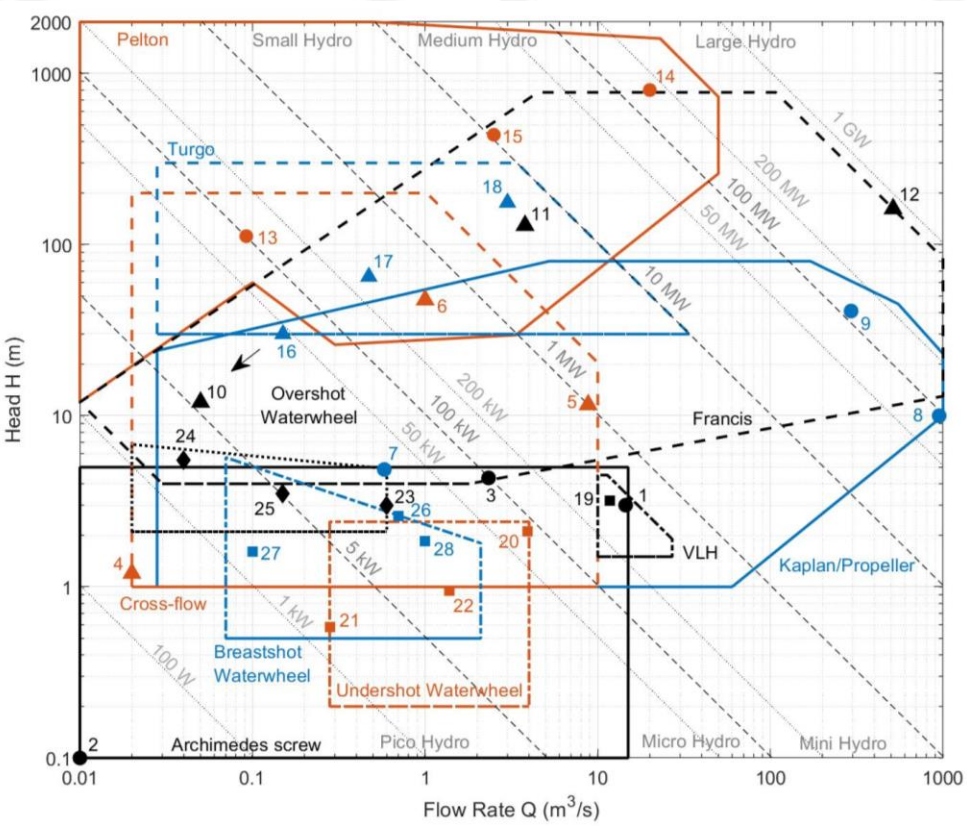

Figure 2: Operational ranges of various hydro-generating technologies. Solid lines indicate the operating envelope, the coloured dots are the operating points of example hydropower plants. Data from various sources [44], [45], [54]–[63], [46], [64]–[68], [47]–[53]**. Index of example power plants are shown in Table A1 of the Appendix.**

The first grid connected ASG in the UK was installed at the River Dart Country Park in Devon, England in 2006. It is a moderately-sized ASG rated to produce 50 kW with a single, variable-speed screw

[69]. The first ASG in North America was installed in Waterford, Ontario, Canada in 2013. It is rated at 7.2 kW with a single, fixed-speed screw and river-to-wire efficiency of about 60% [70]. Table 1 shows examples of ASG installations across the typical size range of ASG plants.

Table 1: Example parameters of real-world installations ranging from a relatively small plant (Fletcher's Horse World) to the largest plant in the world (Linton Lock extension - Widdington) at time of construction. (All photos by authors.)

Location	Rated Power (kW)	Number of Blades (-)	Outer Diameter (m)	Length (m)	Rotation Speed (RPM)	Inclination Angle (°)	Design Head (m)	Flow Rate Capacity (m^3/s)	Site
Fletcher's Horse World, Waterford, Ontario, Canada	7.2	3	1.4	4.5	Fixed (40.7)	22	1.7	0.54	
River Dart Country Park, Ashburton, Devon County, England	50	3	2.2	11	Variable (~31.9)	22	4.5	1.18	
Valpagliaro Plant, Ferrara, Emilia-Romagna, Italy	2 x 121	4	3.6	7.4	Variable (~22.3)	22	3	2 x 5.5	
Romney Weir, Windsor, Berkshire, England	2 x 157	5	4	6	Variable (~45)	Variable (~22)	2	2 x 10.4	
Linton Lock, Linton-on-Ouse, York, England	101	4	3	8.5	Variable (~24.5)	22	3.2	4.5	
	355	4	5	8.5	Variable (~20)	22	3	14.5	

Multiple screws may be installed in parallel at high flow, low head sites. The Valpagliaro plant has two large screws (one fixed- and one variable-speed) that produce up to 121 kW each. The screws have

identical geometry and operate with river-to-wire efficiencies between 70 % to 88 % [71]. The Romney Weir site also has two parallel screws (with identical geometries); each produce up to 157 kW [72] with flow rate capacities of 10.4 m^3/s. In October 2017, a second screw plant was installed at Linton Lock (UK) with a 5 m diameter (355 kW, 14.5 m^3/s) – this unit was the largest ASG in the world at time of construction [73]. More than two screws have been installed at a few sites. Six parallel 30 kW screws, each with 1.4 m head and 3 m^3/s discharge, were installed at the Steinsau weir on the River Ill near Erstein, Alsace, France [74].

3.2. Environmental impacts of ASG installations

ASGs are ordinarily installed in run-of-river (diversion) schemes, recognised as more environmentally friendly than conventional, impoundment hydropower plants. Impoundment systems are often linked to negative environmental impacts such as blocked fish migration and extinction [75], [76], nutrient- and sediment-starved waterways [77], reduced levels of dissolved oxygen [77], greenhouse gas emissions[78]–[81], thermal stratification and shock [82], [83], and mercury methylation [84], [85]. The dam and reservoir, actively controlled to optimize electrical and water supply demands, is often the primary source of these negative impacts.

In a run-of-river scheme no land is flooded for a reservoir, water is neither actively stored nor released over time, fish and sediment passage is impacted but not completely blocked through the main watercourse, and some water always bypasses the hydro plant [86]. Care must still be taken when developing and constructing a run-of-river project since bad practices can introduce tangible environmental impacts [86].

The Archimedes screw itself generally has less impact on fish and aquatic fauna than other pumps or turbines. Screw pumps have been implemented as fish pumps and studies have shown that they

operate with no statistically significant mortality rates – less than 1% of fish showed physical effects (i.e. descaling) from passage through a screw [87], [88].

A neutrally buoyant sensor package was used to measure physical and hydraulic forces experienced by fish during passage through an ASG. Minimal shear forces were observed and no rapid spatial changes in pressure occurred [89], though slight scale loss in fish indicate shear is prevalent [90]. As such fish did not experience high levels of decompression in an operating ASG. However, aquatic wildlife could be struck by screw blades while entering the screw. ASGs rotate slowly (usually 20 to 80 RPM [70]) and fish generally experience minimal trauma entering a screw. However, small fish could experience a pinch-point at the screw inlet [91]. Pauwels et al. [90] observed mortality rates are species specific. Injury and mortality rates are not substantial for eel [90], [92], trout, and salmon [91], [93].

Very large screw pumps/generators have specific features which are usually excluded from installations due to the risk they might pose to aquatic wildlife (i.e. blade leading edges are usually inset to the trough to remove pinch-points, etc.) [94]. Pauwels et al. [90] found low mortality rate in eels, but much higher mortality rates for roach and bream (19% and 37%, respectively) [90]; however, the authors' indicate it was not clear where trauma originated, and site-specific geometry was not available. Trauma has been minimized by installing compressible leading edge bumpers [93] (Figure 3); installation is recommended screw tip speed exceeds 3.5 m/s [95]. However, recent studies found some injury is not caused by leading edge impact, and further investigation is needed to determine these other causes [90].

Figure 3: View inside the forebay of the Ruswarp Hydro ASG. Blade leading edges have rubberized bumpers to minimize impact damage to aquatic fauna.

Kibel found fish were not disoriented after passage and there was no increase in predation downstream [91], [93]; however, another study did observe an increased presence of predators downstream [92]. Downstream migration of Atlantic salmon smolts [96] and silver eel [92] were not markedly delayed by the presence of an ASG installation. While upstream migrating fish like salmon and sea trout were attracted to the screw outflow, none tried to ascend nor jump at the screw, so upstream migration was not hindered [91]. Altogether, available literature supports that ASGs are a "fish-friendly" hydropower option, but there is room for improvement.

3.3. Maintenance and Design Considerations

Regular maintenance regimes are less involved for ASGs than for other turbine technologies [97]. Normal maintenance cycles include trash rack cleaning, regular fluid level checks, and replacement of the upper bearing grease cartridge (if equipped). Some sites exhibited algal growth on the screw blades which reduced power output; seasonal blade cleaning mitigated this issue [98]. Screws may be roofed over and can be built with underflow or curtained inlets and outlets (cf. Fletcher's, Table 1) to prevent algal growth, icing and noise emissions. The Fletcher's screw has operated reliably and without icing issues at temperatures as low as -30 °C.

Routine refurbishment occurs after an expected lifetime of 20 to 30 years [99]. The screw is removed, and its blades are re-tipped while the trough is either replaced (if a metal insert) or repaired (if concrete). Upper and lower bearings are replaced when the screw is reinstalled [97]. This is the only major maintenance cycle required, provided no premature equipment failures occur in components like the generator or gearbox.

Since most ASGs are installed as run-of-river schemes, wide-ranging water levels and flooding events must be considered. Most plants are designed to accommodate some flooding in the powerhouse without damaging equipment. Gearboxes and generators may be arranged to allow higher interior flood levels. The ASG at Goldsborough (UK), where local flood levels can be high, utilizes a "snorkel" design with a watertight generator housing and elevated ventilation shafts to protect equipment (cf. Figure 4).

(a) (b)

Figure 4: Left (a): Goldsborough Archimedes screw generator plant with watertight generator house and dual ventilation snorkels. A fish ladder is adjacent to the right (bank) side of the ASG. Right (b): sign noting interior high-water level at the Ruswarp ASG power house.

ASGs perform more efficiently with partially submerged outlets (around 60%) [100]–[102]. Most screws have fixed inclination angles, but a few (e.g. Romney Weir site) use large hydraulic cylinders to raise or lower the end of the screw (changing inclination angle and relative outlet water level) to capitalise on this efficiency advantage. This functionality allows direct investigation of the optimum

operating inclination angle. At the design stage, optimum inclination angle is important since the length of a screw will depend on the site head and the desired inclination angle [103].

Finally, ASG performance depends partly on the fill level of each bucket. Detail A in Figure 1 shows the variables that define the fill level of an ASG. These can be used to calculate non-dimensional bucket fill height ratio (*f*):

$$f = \frac{z_{wl} - z_{min}}{z_{max} - z_{min}} \quad (1)$$

where z_{min} is the lowest point on the helical plane downstream and z_{max} is the "maximum" water level in a static bucket before overflowing begins [104]. Songin [102] and Nuernbergk [105] give methods for determining the precise values of z_{min} and z_{max} for the unique geometry of Archimedes screws. If $f < 1$, the bucket is partially full of water. If $f = 1$, then the bucket is full and not yet overflowing, while if $f > 1$, the bucket is experiencing overflow leakage.

The fill height of a bucket is dependent on flow rate and rotation speed. Screw generators tend to operate most efficiently at values around $f = 1$. ASGs can be operated at variable speed to increase power production and maintain higher efficiency values. Speed is usually regulated in variable speed systems according to the forebay depth, flow rate sensor readings, or power production values.

Variable speed systems require the generator power output to be rectified so the control system can adjust speed controller frequency. The output signal must then be inverted for on-grid energy usage. This process can potentially incur additional river-to-wire efficiency losses up to about 10% [98], [106] compared to fixed-speed ASGs. The efficiency reduction is offset by the wider operating range of the ASG, and generally, increases in efficiency are much higher than the loss. Some ASGs mitigate variable speed conversion losses by bypassing the speed controller when the ASG is operating at full speed with full buckets [98], [106].

4. Design of an ASG installation

ASG plant design is a complex process, which can be supported by using screw performance models to forecast the impact of various geometrical parameters and operating conditions.

4.1. Geometry and Operating Parameters

Figure 1 defines the geometry of an ASG; a three-bladed (or "three start", $N = 3$) screw is shown. Screws with three or four blades are most common. Five blade screws (e.g. Romney Wier, UK) [103] and two blade screws (e.g. Cragside, UK) are less common. Theoretically, a higher number of blades is more efficient [1]; however, there is a realistic limit once thickness and frictional effects are considered. Laboratory-scale experiments and computational fluid dynamic (CFD) techniques found a five-bladed screw was slightly more efficient then otherwise geometrically identical screws three or four blades [101][103]. Practically, five blades seem to be the real-world maximum due to manufacturing difficulty and negligible net power returns from additional blades.

The most common ratio of inner to outer diameter in screw pumps is $D_i/D_o \approx 0.5$ [107]. The theoretical optimum is closer to 0.54 [1] but this does not account for losses. Experiments suggest that this ratio is appropriate for ASGs [41], [101]; this has been confirmed using Bayesian optimisation techniques [108].

ASGs commonly have pitch-diameter ratios of $S/D_o \approx 1.0$ [41], [107]. Laboratory-scale experiments with pitch ratios (S/D_o) of 0.80, 1.00 and 1.41 found that the screw with $S/D_o = 1.0$ was most efficient; though the results were not statistically significant [102].

ASGs operate at very low rotation speeds relative to other turbines (10 to 125 RPM [41]); most commonly around 30 RPM [109]. As with diameter ratio, screw pump rotation speeds are similar to ASGs. The empirical relationship for maximum practical screw pump rotation speed (termed the "Muysken limit") is [110]:

$$V_M = \frac{50}{D_o^{2/3}} \quad (2)$$

where units of D_o must be meters and V_M is RPM. Equation (2) yields incorrect results for laboratory-scale screws (i.e. 10 W to 100 W screws); however, it is a reasonable estimate for practical power plant sizes [41]. Nuernbergk [105] reviews rotation speed guidance in more detail.

ASGs can be classified by flighted length to pitch ratio (L/S) which can be interpreted as the number of turns of a screw along its length. This ratio is used to classify if a screw is "short" or "long". Similarly, the average number of buckets (n_b) in an operating screw is

$$n_b = \frac{N \cdot L}{S} \quad (3)$$

In practise, L/S varies widely. Laboratory-scale screws have been tested between L/S = 1.16 and 4.8 [102]. The length of a real-world screw is usually based primarily on inclination angle β and available hydraulic head ΔH with pitch-to-length a secondary criterion. In real-world ASGs, L/s is commonly between approximately 1.5 (Widdington, UK) and 5 (Buckfast Abbey, UK and River Dart, UK). The head across an ASG is:

$$\Delta H = L \sin \beta + h_U - h_L \quad (4)$$

if the upper water level (h_U) and lower water level (h_L) are known (cf. Figure 1).

Inclination angles between 22° to 26° are common at real-world ASGs with some extreme values (i.e. 30°) [38], [111]. In design practice, inclination angle is often specified, and screw length is adjusted to satisfy on-site available head conditions. This can yield extremely long screws. A 12 kW ASG in Cragside, United Kingdom has N = 2 flights and length L = 15 m to accommodate a comparatively large 8.3 m head and very low flow rate (Q < 1 m^3/s) [112].

Laboratory-scale experiments provided evidence that increased screw length corresponded to increased efficiency; however, this might not be true for larger real-world screws [101]. Longer screws have more surface area to convert hydraulic- to mechanical power, however, there are increased frictional losses, so that an excessively long screw may be less efficient. More material is required to ensure sufficient stiffness in longer screws, while gap width increase to account for deflection. Conversely, short screws operate less efficiently since there is less length for buckets to fully form as they translate down the trough. The impacts of inlet and outlet losses are proportionally magnified when efficiency is calculated. Thus, there will be a practical optimal screw length to balance these factors. An optimal length was not conclusively found in laboratory-scale experiments of several screws identical except for length [113] and definitive guidance is unavailable for full-scale screws due to the many dependent variables.

Screws with low inclination angles performed best in a study that varied length and inclination to maintain a constant head: three inclination angles were tested (15.6°, 24.4°, and 33.8°) and the screw with β = 15.6° had the highest efficiency [113]. The authors plan to extend their dataset with CFD simulations to test these relationships further, since existing literature on inclination angles suggests the opposite [103], [114]. There is a practical trade-off in selecting an inclination angle. For a given head, decreasing inclination angle requires increasing length, which means more material is required for the screw, frame, and possible changes to bearing arrangement. This is likely the reason that many ASGs have inclination angles of 22° [41], as in practice this seems to offer a good balance between performance and cost.

4.2. Experiments and Site Studies

Over the last decade, more experimental studies and site assessments of ASGs have been added to the literature (Table 2), making further model development more feasible.

Table 2: Dimensions and operating parameters of some ASG experimental studies. The authors were unable to find further details for the works of Anzawa et al. (2017), Adhikari et al. (2016), or Johnson (2018), however an approximation for the scale of their experiments (an estimate of the outer diameter) has been made in lieu of this.

Publication	Location	D (m)	L (m)	N (-)	β (°)	Q (L/s)	ω' (RPM)	P (W)
Saroinsong et al., 2015	*Brawijaya University, Malang, Indonesia*	0.11	0.924	3	30	~0.5	50 to 300	~1
Erinofiardi et al., 2017	*University of Bengkulu, Bengkulu, Indonesia*	0.142	0.646	1	22 to 40	1.2	106 to 225	1.4
Lubitz et al., 2014	*University of Guelph, Ontario, Canada*	0.15	0.6	3	24.5	0.755	25 to 200	1.2
Dellinger et al., 2016	*ICUBE Laboratory, Strasbourg, France*	0.192	0.4	3	18 to 30	1 to 4	60 to 180	6
Straalsund et al., 2018	*Pacific Northwest National Laboratory, Washington, USA*	0.19914	0.766	4	20.6 to 29.1	10 to 210	1 to 5.8	2 to 12
Siswantara et al., 2019	*Universitas Indonesia, Depok, Indonesia*	0.3	2.09	2	36 to 44	1.06	84.2 to 113.3	20 to 40
Anzawa et al., 2017	*Nippon Koei Co., Ltd., Sukagawa, Japan*	No Data (~0.3)	No Data	No Data	No Data	No Data	No Data	No Data
Adhikari et al., 2016	*Institute of Engineering, Lalitpur, Nepal*	No Data (~0.2)	No Data	No Data	40	0.3 to 0.5	No Data	No Data
Songin and Lubitz, 2018	*University of Guelph, Ontario, Canada*	0.32 to 0.38	0.41 to 1.22	3 to 5	15 to 33	6 to 14	20 to 80	6 to 60
Lashofer et al., 2013	*University of Natural Resources and Life Sciences, Vienna, Austria*	0.806	3	3 to 5	18 to 32	20 to 220	20 to 80	~3000
Rohmer et al., 2016	*ICUBE Laboratory, Strasbourg, France*	0.84	1.4	3	30	50 to 400	0 to 85	3000
Brada, 1999	*Czech Technical University, Prague, Czech Republic*	1.05	4.7	3	30	233 to 316	54.7	4000
Kozyn et al., 2018	*Fletcher's Horse World ASG, Ontario, Canada*	1.39	4.53	3	22	536	44.5	7200
Johnson et al., 2018	*Utah State University, Utah, USA*	No Data (~2)	12.8016	4	25	280 to 1560	No Data	35000
Fergnani and Silva, 2015	*HydroSmart Srl, Ferrara, Italy*	3.6	7.4	4	22	5500	22	121000

Nuernbergk [100], [105] presented a complete work outlining theories and applications of ASGs. One section documented experiments carried out at the Czech Technical University in Prague [115] and at the University of Natural Resources and Life Sciences in Vienna [116]. Brada (1999) pioneered research on Archimedes screws for hydropower production. A 4 kW test screw was installed on the River Eger in Aufhausen, Germany and provided some of the first evidence for the viability of ASGs for hydropower production [115]. Lashofer et al. (2013) tested a small, real-scale ASG in a laboratory to characterize its efficiency as a function of flow (Q = 20 to 220 L/s) and rotation speed (Ω = 20 to 80 RPM) while varying the inclination angle at increments of 2° from β = 18° to 32° [116].

Experiments on small laboratory-scale screws at the University of Guelph (Canada) to inform development of a performance model for ASG power production [104]. Further experimental data, and

site data from the Waterford (Fletcher's) ASG (cf. Table 1) aided development of power loss prediction models [70], [117]. Further tests were conducted on 16 unique, laboratory scale ASGs – the resulting data was analysed in different ways to isolate the effects of specific parameters on performance [101], [102], [118], [119]. The apparatus also allowed adjustment of inclination angle [113], [120], addition of an inlet channel modification [121], and tests of screw pump performance [122].

Laboratory-scale ASGs were tested at the ICUBE Laboratory at INSA Strasbourg. Rohmer et al. (2016) compared experimental results from the largest laboratory-scale screw (at time of study) against model predictions, and suggested improvements to modelling techniques [123]. Dellinger et al. (2016) used experimental results from a smaller laboratory screw to evaluate the accuracy of a CFD model that was then used to investigate ASG parameters that are difficult to vary in full- or laboratory-scale screws [124], [125].

A few independent studies varied discharge and inclination angle in laboratory-scale screws to suggest the optimum ASG inclination angle [114], [126], [127]. A follow-up study observed gap leakage and fluid motion in screw buckets through a transparent trough during operation [128]. Anzawa et al. experimented on a laboratory-scale ASG to aid in the design of efficient control devices for a wide range of operating conditions [129].

Different end treatments have been tested to reduce noise and minimize outlet losses [8]. A full-scale screw was built in-laboratory and tested across a range of flow rates and other operating parameters [130], however, the study results were not published.

The literature contains data from full-scale ASG powerplant site assessments [70], [100], [105], [115], [119], [131], [132], with the survey work of Lashofer et al. being particularly notable [38]. However, measuring parameters like the flow rate and bucket fill height is difficult in operating full-scale ASGs, which limits the usefulness of these assessments for model advancement.

Some authors have presented design, development and implementation of rural, off-grid systems in developing regions in the world. Dhakal et al. experimented on a small-scale ASG to evaluate feasibility for installation in Nepal [133]. Okamura et al. outline the design, development, and implementation of an ASG system in southern Tanzania [134].

An ASG powerplant along the Apfelstädt river in Herrenhof, Germany was instrumented to test relationships between discharge, head, rotation speed, and power production [135]. Similar work was performed at a powerplant in Mühlen in Taufers, Italy. The variable-speed installation was used to test efficiency at different rotation speeds [135]. The Valpagliaro plant near Ferrara, Italy was well instrumented and resulting literature includes discussions of site design optimization [136], efficiency and power production assessment [132], and site-specific economic assessments [137].

Though many of these studies present data collected from these full-scale sites, it remains difficult to utilize the data for modelling purpose, because all variables included in the model must be known simultaneously to quantify the performance of the model against the measured data. Future model development requires comprehensive data from a larger set of installations.

4.3. Parametric Models

Design and optimization of ASG installations can be enhanced by using one of several parametric models presented in the literature. Some modelling techniques have been used to simulate screw performance in larger energy systems [138]. Müller and Senior [139] presented a simplified model for ASG performance; it is too simplified for practical implementation in detailed plant design.

Nuernbergk [100] presented a broad performance model that includes many details for screw design, analysis, and modelling. This text remains the most comprehensive single source on ASGs; a second edition was recently published [105]. Lubitz et al. [104] developed an ASG performance model utilizing analytical relationships and numerical integration to predict power production and efficiency.

Gap and overflow leakage losses were included. Further updates include power loss models for bearing friction, outlet expansion, hydraulic friction, and outlet submersion [117]. Rohmer et al. [123] presented a model that predicts ASG performance and accounts for gap leakage losses, overflow leakage losses, and frictional effects to improve model accuracy. These models are broadly similar. Bucket water volumes and torque due to static pressure on blade surfaces are calculated and various corrections are applied to account for inlet and outlet losses, friction losses, and efficiency losses from gap and overflow leakage.

4.4. Inlet Loss Modelling

Determining the correct screw inlet elevation relative to upper reservoir depth is important in site-specific ASG design. The literature contains models to predict upper water level (h_U) given various design and operational parameters. Nuernbergk and Rorres [140] used discharge (Q) to predict upper water level and account for inlet channel losses. Most inlet hydraulic losses are due to the geometry change between the inlet channel and the screw entrance. Nuernbergk and Rorres adapted the Borda-Carnot head loss relation to account for the geometric change from a rectangular cross section inlet channel, to the tilted circular cross section of the screw and trough [140]:

$$h_U = h_2 + \frac{1}{2g}\left(\frac{Q}{h_2 b_2}\right)^2 \left[1 + \zeta_U - \left(\frac{h_2}{h_1}\right)^2\right] \quad (5)$$

Here, h_1 and h_2 are channel- and screw entrance-specific water levels, b_2 is the inlet channel width, Q is flow rate, g is the gravitational constant, and ζ_U is the hydraulic loss factor. Borda-Carnot head loss from a rectangular to a tilted circular cross section was used to approximate $\zeta_U = 0.119$ [140]. Note this model does not account for screw rotation speed. A simple empirical, predictive model developed from experimental data found that the upper water level of ASGs is dependent on both flow rate and rotational speed [121]. Additional validation of inlet loss models is needed.

4.5. Outlet Loss Modelling

There are two major types of outlet losses discussed and modelled in the literature: outlet expansion ($P_{L,OE}$) and outlet submersion losses ($P_{L,OS}$) [70].

At the screw outlet, water passes from a tilted circular cross-section to the larger cross-section of an outlet channel or reservoir – giving rise to expansion losses. Most full-scale ASGs have short channel extensions at the outlet to house stop logs during maintenance operations; however, these also reduce outlet expansion losses [98]. Outlet expansion losses have been modelled using equation (6) [70].

$$P_{L_{OE}} = \rho Q \zeta_L \frac{v_t^2}{2} \tag{6}$$

where ζ_L is the Borda-Carnot exit loss coefficient. Kozyn and Lubitz (2017) provide more details on this loss coefficient, noting approximately $\zeta_L < 1$ [70]. Transport velocity (v_t) is defined as:

$$v_t = \frac{S\omega}{2\pi} \tag{7}$$

This is the speed that buckets translate along the trough, and so is dependent on screw pitch and rotation speed (ω).

Outlet submersion losses (or losses from non-optimal lower water level [100]) are more significant than outlet expansion losses. Experiments showed that power output varied significantly with changing lower water level (h_L) [43]. In practice, while lower water levels are site-specific, the screw should be installed at a height to optimise performance. The dimensionless lower water level is

$$\Psi_L = \frac{h_L}{D_o \cos\beta} \tag{8}$$

ASGs with Ψ_L = 60% were most efficient in laboratory experiments [102]. The outlet water level provides back pressure on the last bucket in the screw; without this pressure the last few buckets of the

screw drain prematurely. Conversely, when the lower water level was too high, the last few buckets were flooded from below. Optimum lower water level (h_L') for a screw operating full (f = 1) is modelled as [105]:

$$h_L' = \left(\frac{D_o + D_i}{2}\right)\sqrt{1 - \left(\frac{S\tan\beta}{\pi D_i}\right)^2}\cos\beta - \frac{S}{N}\sin\beta \quad (9)$$

The balance between flooding and draining seems to be met around Ψ_L = 55% to 60% [100]. Outlet submersion power loss is then predicted when $h_L > h_L'$ [105],

$$P_{L_{OS,\ high}} = \rho g Q \frac{(h_L - h_L')^2}{h_L} \quad (10)$$

and when $h_L < h_L'$ [105].

$$P_{L_{OS,\ low}} = \rho g Q \frac{(h_L - h_L')^2}{h_L'} \quad (11)$$

Lab experiments and field data suggested this model overpredicted power loss when $h_L < h_L'$ and has inaccuracies when $f \neq 1$ [119]. An empirical loss coefficient was implemented to improve model predictions for cases with f = 1; this correction might only be applicable to small, laboratory-scale screws.

An empirical model based on lab-scale experiments was developed to predict outlet submersion losses [70]. This model assumes outlet submersion losses depend on lower water level, discharge, and rotation speed.

Blade impacts at the inlet and outlet of ASGs generates noise during operation [100], [141]. While this is usually at acceptable levels, in some cases site owners may seek to reduce noise to appease neighbours and reduce outlet losses [41]. Some ASGs have modified blade end treatments to aide in

noise reduction. Figure 5 shows a screw with a v-notched trailing edge [98], [142]. Though noise is reduced, the final buckets drain prematurely introducing a new loss.

Figure 5: Modified blade ends at the Goldsborough ASG outlet.

Other geometry modifications have been proposed to improve performance. For instance, the helical flights may be joined to the central cylinder at angles other than the standard 90°. Experimental tests of this modification found significant performance improvements only occurred at high speeds and were likely due to dynamic effects during bucket filling at the inlet [8].

4.6. Frictional Losses

Hydraulic friction may be modelled by components in the transport (axial) direction and rotational direction (counteracting torque) [70]. The Darcy-Weisbach equation, Manning's equation, and relationships discussed in Nuernbergk [100] were used to develop a numerical solution for hydraulic friction [70]. Further development seems required to improve predictions of surface roughness effects. Independent reports contend that significant algal growth on screw blades caused power losses of about 11% [98] and 10% [143] relative to clean, algae-free operation in two different full-scale ASGs. This suggests that surface roughness is an important factor in ASG performance; further investigation is required.

4.7. Gap Leakage Losses

ASGs have a small gap between the trough and rotating blade edges to allow the screw to turn freely (cf. Figure 1). This gap width is minimized to reduce leakage between successive buckets. In

practice, many ASGs are designed using an empirical screw pump relationship [107] to estimate an appropriate gap width:

$$G_w = 0.0045\sqrt{D_o} \tag{12}$$

In practice, the width of the gap region tends to differ from the designed size. Changes in screw water levels effect buoyancy, changing deflection patterns in the screw and the gap width along the screw's length, by extension. Imperfections in the steel construction and paint can alter the gap width. As well, wearing of components can alter the gap width. Bearings wear as they operate over more cycles. In particular, as journal bearings wear the axis of rotation tends to shift noticeably. The screw blades and trough may also experience wear due to sediment transport. Current modelling techniques approximate the gap width and assume it to be constant throughout the length of the screw.

The total discharge (Q) of an ASG consists of bucket flow (Q_b), gap leakage (Q_g), and overflow leakage (Q_o):

$$Q = Q_b + Q_g + Q_o \tag{13}$$

Overflow leakage is the rate of water over-topping the inner cylinder and flowing into the next bucket. Both gap and overflow leakage do not contribute significantly to torque generation. Both are subtracted from total flow to yield the bucket flow rate; the discharge corresponding to torque generation.

For screw pumps there is an empirical model [107] and a first principles model [1], [110] to predict Q_g; the first principles model was later adapted for ASGs [140]. It uses the installation geometry of the installation, bucket water level, and a discharge coefficient to predict the gap leakage flow rate. A similar first principles model was cast in terms of wetted arc-lengths [144]. These two models are functionally similar, so the latter will be discussed further since it was experimentally evaluated [117]:

$$Q_g = C G_w \left(l_w + \frac{l_e}{1.5} \right) \sqrt{\frac{2gS}{N} \sin \beta} \tag{14}$$

Here, C is a hydraulic loss coefficient that is set to unity if minor losses are neglected. A value of C = 0.89 is sometimes used in practice [144]. The wetted length of the constant pressure portion of the gap (l_w) and the total length of the gap region (l_e) (cf. Section B, Figure 1) are calculated numerically based on screw geometry.

The current gap leakage models do not account for the important variable of rotation speed. A numerical study showed that as screw rotation speed increased the relative flow velocity through the gap decreased (Figure 6) [145], [146]. It was theorized that the relative velocity through the gap would continue to decrease until the blades "outran" the leakage rate (i.e., transport velocity exceeded gap flow velocity); corresponding to negative gap leakage [145].

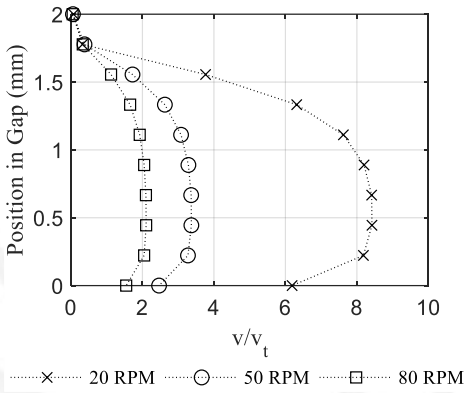

Figure 6: Relative velocity of water through the gap region of a laboratory-scale screw [146] **for different transport velocities. The vertical axis indicates the radial position of the sample point within the gap vertically, where 0 mm is located on the bottom of the trough and 2 mm is at the blade tip (i.e. gap width is 2mm).**

Figure 6 lends credence to the aforementioned theory. Future gap model development should incorporate rotation speed. The above first principles models could perhaps tune the hydraulic loss coefficient to account for this phenomenon.

4.8. *Overflow Leakage Losses*

Overflow leakage passes through a triangular cross-section, consequently, models presented in the literature are adapted from triangular weir equations [104], [123], [140], [147]:

$$Q_o = \frac{4}{15}\mu\sqrt{2g}\left(\frac{1}{\tan\beta} + \tan\beta\right)(z_{wl} - z_{max})^{5/2} \tag{15}$$

where g is the gravitational constant (9.81 m/s^2) and μ is a coefficient usually set to μ = 0.537 [100], [147]. However, a value of μ = 1.0633 was suggested in [123] to account for kinetic energy and surface velocity distribution. Eq. 15 is only valid if z_{wl} exceeds z_{max} (i.e. $f > 1$).

Songin and Lubitz [118] suggested extending Eq. 15 to account for shear stress and surface current effects. This resulted in a model overflow for laboratory-scale screws:

$$\frac{Q_o}{Q} = \begin{cases} 1.085\left(\dfrac{\frac{4}{15}\mu\sqrt{2g}\left(\frac{1}{tan\beta} + \tan\beta\right)(z_{wl} - z_{max})^{\frac{5}{2}}}{Q}\right) + 0.238\omega_{nd} & f > 1 \\ 0 & f \leq 1 \end{cases} \tag{16}$$

Here the rotation speed is non-dimensionalised by the Muysken limit (equation (2)) to yield ω_{nd}. Equation (16) was shown to improve model accuracy experimentally, but further development is required to make it applicable to full-scale ASGs [102].

4.9. *Dynamic Flow Phenomena*

Waves on water surfaces in buckets have been observed by the authors in experiments [101], during site visits, and in simulations [148]. Waveform development seems chaotic. As a bulk flow, a "sloshing" phenomenon was observed that led to overflow in only some buckets along the screw length. An example of uneven bucket filling along a screw is visible in the CFD results of Dellinger et al. [149] (Figure 7).

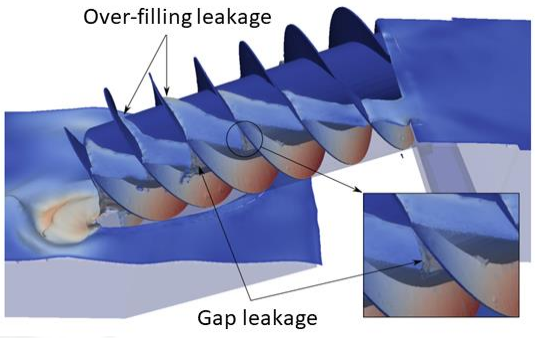

Figure 7: Visualization adapted from Dellinger et al. [149] **showing a D_o = 0.192 m ASG with an uneven bucket fill pattern for a flow rate of Q = 2.8 L/s, rotational speed of 70 RPM, and inclination angle of β = 24°.**

The authors theorize that these patterns of varying fill with length are an artifact of the process of water filling and initial bucket formation at the ASG inlet. It was originally theorized that the uneven bucket water level distribution was due to imperfections in the screw during manufacturing (varying gap width, bucket width); however, the appearance of this phenomenon in a geometrically perfect CFD simulation indicates that is not the case. As the blades rotate, water rushes into each bucket as it forms with significant momentum. In a static system, water would slosh back-and-forth in an enclosed bucket until the oscillations equilibrated. So, in an operating screw, the water sloshes as the buckets translate down the screw – causing variable fill levels related to the bulk volume "sloshing" frequency. This phenomenon may have an impact ASG performance and would be valuable to quantify.

Quantifying this phenomenon experimentally is difficult. Since a screw is a fully enclosed system with rotating helical blade faces it is difficult to use Particle Image Velocimetry (PIV) techniques to quantify fluid motion in the screw's buckets. CFD offers a potential solution to this problem, although analysis of this problem has not been located in the literature.

4.10. Computational Fluid Dynamic Models

CFD has been used to investigate variations in ASG performance due to changes in pitch [150], number of blades [120], [150], flow rate [133], [151], outlet variations [152], pressure and velocity characteristics [125], [150], and inclination angle [120], [133], [148], [151], [153]. Numerical simulations

in the literature include simulations of single buckets and multiple coupled buckets [145], [146], as well as full-scale dynamically meshed domains [125], [148], [151].

Full-scale dynamically meshed ASG simulations are the most computationally expensive CFD models, but these can provide the most insight for general model development. For example, further efforts to model predictions applicable for both laboratory- and powerplant-scale ASGs are underway using a full-scale CFD model [148]. However, due to computational constraints, other domains may be appropriate. Modelling gap leakage, for example, required high levels of mesh refinement in the gap region; this was accomplished by simulating a single- and multiple-coupled-bucket domain to quantify effects with and without gap leakage [146].

CFD studies of ASGs provide valuable insights for future performance model developments. A validated numerical simulation provides accurate approximations of ASG performance characteristics and allows researchers to explore the performance and specific phenomena in any imaginable ASG design without the costs associated with traditional experiments or field work.

5. Economics of Archimedes screw generators

Archimedes screws have a simple, robust construction with minimal requirements for difficult, high tolerance fabrication. Consequently, it is possible to produce simplified ASGs with local resources in remote, off-grid communities, or as an inexpensive option for on-grid energy production. Figure 1 illustrates the main components of an ASG system, which include a trash rack, sluice gate or stop logs (to control intake level and flow), gearbox and generator, upper bearing, Archimedes screw, trough, lower bearing, plus civil works and electrical components.

ASGs require a screen (commonly termed “trash rack”) upstream of the screw to prevent entry of large debris (i.e. floating logs, etc.). However, very coarse screens suffice (i.e. 100 mm openings [95])

since sediment, debris, and even fish may pass through the screw unharmed due to the robust design, low rotation speed, and large interior spacing in ASGs [87], [89], [93].

A gearbox or other transmission converts the low screw rotation speed to standard generator speeds (750 RPM to 1800 RPM). Most other hydropower turbines operate at high speeds and do not require a gearbox, so this is an additional installation and maintenance cost associated with ASGs. However, the overall cost of installation and maintenance of an ASG powerplant is low compared to other technologies [154].

For a specific UK site, it was found an ASG would produce about 15% higher energy output for 10% less cost than a comparable Kaplan turbine; the ASG was 22% less expensive per MWh [154]. However, it should be noted that the optimal choice of technology is highly site-specific. Generally, ASGs have low civil construction costs because they are often retrofit to existing infrastructure such as an old mill site or flood control dams and require different powerhouse structures than more common hydropower technologies [99].

ASG maintenance and operating costs are also comparatively low [155]. The main wearing components are the bearings, screw blades, and trough, but there are fewer wearing cycles per unit time than in other turbines due to low rotation speeds. The lower bearings are designed to operate fully sealed and lubricated with minimal maintenance requirements. Screw manufacturer Spaans Babcock Hydro Power suggested a 30 year lifetime for a screw [99]. Many screw plants have slotted civil works that extend past the screw outlet so a temporary stop log system can be inserted to dry out the lower portion of the screw during bearing maintenance.

Operating costs of a micro-hydropower installation also vary with plant size. A 25 kW plant may have an annual operating cost of 4000 GBP (6120 USD) per year, while a 500 kW installation may cost 48300 GBP (73900 USD) per year. Archimedes screws should have lower operating costs than this

555 estimate since their intake screening requirements are much coarser than other hydroelectric
556 technologies [156].

557 In a survey of site owners and operators, Lashofer et al. found that specific investment costs ranged
558 from 0.5 to 2.2 €/kWh (0.64 to 2.82 USD/kWh, exchange rate at time of study) [41]. A 25 kW plant was
559 estimated to cost 169 000 GBP (259 000 USD, exchange rate at time of study), or 6800 GBP/kW (10 400
560 USD/kW), while a 500 kW plant was estimated at 1.6 million GBP (2.45 million USD), or 3200 GBP/kW
561 (4900 USD/kW) [157]. Relative plant costs decreased as plant size increased.

562 A 260 kW hydropower project (constructed in Kilnhurst, UK, 2015) that utilized a pair of Archimedes
563 screws had an estimated project cost of 3.25 million USD [158], including measures to improve aquatic
564 wildlife passage up- and downstream of the installation.

565 A feasibility study proposed that a single 150 kW screw (proposed in London, UK, 2009) would cost
566 848 000 GBP (1 332 000 USD, exchange rate at time study) to install and would incur annual costs of
567 5700 GBP (8950 USD), including annual costs of: 600 GBP for operational costs, 1000 GBP for insurance,
568 1500 GBP for rates, 400 GBP for meter reading, and 2200 GBP for equipment maintenance [159]. The
569 total annual revenue of this single screw was estimated at 124 000 GBP (195 000 USD), yielding a
570 payback period of 7 years assuming a conservative system efficiency of 60%. The payback period
571 decreased to 6 years for a two- or three-screw installation [159].

572 To make investment more manageable, Archimedes screws are well-suited to distributed
573 ownership, or community-based development. Examples include the Whitby Esk Energy hydroelectric
574 plant in Whitby, UK and Torrs Hydro in New Mills, UK. These sites are run by Esk Energy (Yorkshire) Ltd.
575 [160] and Torrs Hydro New Mills Ltd. [161], respectively.

6. Research Needs

The literature does not decisively address the issue of size scaling in ASG power prediction models; models were often developed using primarily laboratory-scale experimentation and may not be applicable to full-scale ASG powerplants. Numerical simulation offers the ability to evaluate and develop models across any scale ASG. As an extension, current leakage models may be revisited since CFD modelling techniques offer novel, quantitative insight into both gap- and overflow leakage.

Inlet loss modelling could be improved by developing a first principles model that incorporates discharge and rotation speed. Quantifying inlet loss is an integral step in optimizing inlet channel design to minimize entrance losses. As well, it may help to determine the height to place the screw inlet within a canal or penstock with respect to the weir crest.

Outlet expansion and submersion losses are currently modelled empirically. A general outlet loss model for all scales of ASGs would assist designers. Improved outlet modelling will aid in optimizing screw design, including further investigation of end treatment effects. Some preliminary investigation was conducted regarding screw length and inclination angle optimization [162], but it was carried out at the laboratory-scale. Further investigation would be beneficial, particularly with respect to manufacturing costs; though it may prove difficult due to their proprietary nature.

Study of the internal fluid mechanics of a bucket using full-scale, transient CFD simulations paired with experimental investigations of the “sloshing” phenomenon (cf. Section 4.9) might aid in quantification of internal shear losses during operation. The “sloshing” effect suggests there is non-negligible kinetic energy within a screw’s buckets that does not necessarily contribute to power production. Knowledge of internal bucket mechanics (kinetic energy and frictional losses) may improve accuracy of current power prediction models.

Discussions with plant operators suggested algal growth on ASG blades exacerbated frictional losses and increased capillary flow during operation, suggesting surface roughness has a significant impact on plant performance. Further study of this phenomenon is required to document and quantify this loss in the literature.

Further investigation into optimizing variable speed operation of ASGs also seems necessary. Variable speed operation was shown to successfully improve plant efficiency [132], as such, the majority of new installations utilize variable-speed operation. However, variable-speed operating system algorithms are proprietary and therefore lacking in the literature.

Finally, many Archimedes screw power plants contain multiple screws. Some power plants with widely varying year-round flow duration curves might benefit from multiple screws; for example, one smaller screw could operate at the base flow and a larger, variable-speed screw could operate during higher flows. As far as the authors are aware, the literature does not contain discussions on optimization of multi-screw installations.

7. Conclusion

Archimedes screw generators are an eco-friendly hydropower technology that are economically viable due to a simple, robust design, low cost of installation and maintenance, and potential range of operating conditions. The technology is appropriate for small-scale hydropower and run-of-river installations. There are many site-specific variations in plant design (e.g. variable inclination angle to cope with tidal variations in lower water level, snorkel design to prevent powerhouse flooding, etc.). Modelling techniques may be used to design an ASG site for specific conditions, provided site data is available for flow rates and water levels.

The recent literature contains a great deal of material useful for the design and optimization of an Archimedes screw generator installation. The redesign and creation of some power loss predicting

models and optimization models would be beneficial to further the accuracy and reliability of Archimedes screw generator design and, by extension, optimally design a powerplant before installation.

8. Acknowledgements

This work is part of larger long-term research program that has been financially supported by the Natural Science and Engineering Research Council (NSERC) of Canada, Collaborative Research and Development (CRD) program (grants CRDPJ 433740-12 and CRDPJ 513923-17) and Greenbug Energy Inc. (Delhi, Ontario, Canada). The authors gratefully acknowledge the efforts of Tony Bouk and Brian Weber of GreenBug Energy Inc. (Canada) for their continued support. The support of David Mann and Adrian Clayton of Mann Power Consulting Ltd. (UK), Chris Elliot of On Stream Energy Ltd. (UK), David DeChambeau of Southeast Power Engineering Ltd. (UK), Mike Ford of Esk Energy (Yorkshire) Ltd. (UK), Guilhem Dellinger of the ICUBE Laboratory (INSA Strasbourg, France), and Nicola Fergnani of HydroSmart Srl (Italy) has been invaluable to this research and is greatly appreciated.

9. References

[1] C. Rorres, “The Turn of the Screw: Optimal Design of and Archimedes Screw,” *J. Hydraul. Eng.*, vol. 126, no. 1, pp. 72–80, 2000.

[2] K.-A. Radlik, “Hydrodynamic screw for energy conversion - uses changes in water supply to regulate energy output,” DE4139134A1, 1997.

[3] S. J. Williamson, B. H. Stark, and J. D. Booker, “Low head pico hydro turbine selection using a multi-criteria analysis,” *Renew. Energy*, vol. 61, no. 0, pp. 43–50, 2014.

[4] “The Taming of the Screw,” *Engineering & Technology*, Stevenage, Oct-2010.

[5] Tees Barrage International White Water Centre, “Tees Barrage,” *tbiwwc.com*, 2020. [Online].

Available: https://tbiwwc.com/. [Accessed: 05-May-2020].

[6] S. Dalley and J. P. Oleson, “Sennacherib, Archimedes, and the Water Screw: The Context of Invention in the Ancient The Context of Invention in the Ancient World,” *Technol. Cult.*, vol. 44, no. 1, pp. 1–26, 2003.

[7] A. Spalinger, “Esarhaddon and Egypt: An Analysis of the First Invasion of Egypt,” in *Orientalia*, Vol. 43., New York: GBPress, 1974, pp. 295–326.

[8] J. L. Straalsund, S. F. Harding, D. M. Nuernbergk, and C. Rorres, “Experimental evaluation of advanced Archimedes hydrodynamic screw geometries,” *J. Hydraul. Eng.*, vol. 144, no. 8, pp. 1–10, 2018.

[9] T. Koetsier and H. Blauwendraat, “the Archimedean Screw-Pump : a Note on Its Invention and the Development of the Theory,” *Proc. Int. Symp. Hist. Mach. Mech. (HMM04). Kluwer, Dordercht*, pp. 181–194, 2004.

[10] A. I. Wilson, “Classical water technology in the early Islamic world,” *Institutum Rom. Finlandiae*, no. January 2003, pp. 115–411, 2003.

[11] L. White Jr., *Medieval technology and social change*. London: Oxford University Press, 1974.

[12] W. G. Nash, *The Rio Tinto Mine: Its History and Romance*. London: Simpkin Marshall Hamilton Kent & Co Ltd., 1904.

[13] Ḥarīrī and Y. ibn M. Wāsiṭī, *Maqamat Al-Hariri*. London: Bibliothèque nationale de France, 2003.

[14] S. Guthrie, *Arab Social Life in the Middle Ages: An Illustrated Study*, 1st ed. Detroit: The University of Michigan, 1995.

[15] K. Kyeser, *Bellifortis*. Eichstätt: University of Göttingen.

[16] L. da Vinci, *Codex Atlanticus*. Florence, 1519.

[17] G. Cardano, *De subtilitate Libri XXI*. Basel, 1584.

[18] A. Ramelli, *Le diverse et arcificiose machine*. Paris, 1588.

[19] G. Galilei, *Opere di Galileo Galilei*. Bologna: per gli hh del Dozza, 1656.

[20] R. J. Hoeksema, *Designed for Dry Feet: Flood Pretection and Land Reclamation in the Netherlands*, 1st ed. Reston: American Society of Civil Engineers, 2006.

[21] F. Hassan, "Water history for our times," *IHP essays water Hist.*, vol. Vol. 2, 2011.

[22] K. Vaughan, "Windmills of Holland," *PSA J.*, no. April, pp. 30–33, 2006.

[23] A. Kozyn, "Power Loss Model for Archimedes Screw Turbines," University of Guelph, 2016.

[24] H. Addison, "Experiments on an Archimedean screw," *Inst. Civ. Eng.*, no. 75, 1929.

[25] A. Poosti and F. M. Lewis, "Pump replacement at the Hyperion Intermediate Pump Station: Analysis of Archimedes Screw vs Vertical Turbine Pumps," Los Angeles, 2002.

[26] E. A. Asli-Ardeh and A. Mohsenimanesh, "Determination of effective factors on power requirement and conveying capacity of a screw conveyor under three paddy grain varieties," *Sci. World J.*, vol. 12, no. 1, 2012.

[27] S. S. Waje, B. N. Thorat, and A. S. Mujumdar, "Hydrodynamic Characteristics of a Pilot-Scale Screw Conveyor Dryer," *Dry. Technol.*, vol. 25, pp. 609–616, 2007.

[28] FishFlow Innovations, "Fish Friendly Screw Pump: Pump as Fish Passage," *fishflowinnovations.nl*, 2019. [Online]. Available: http://fishflowinnovations.nl/en/innovations/screwpump/#1483537045652-5ec9b0e6-032c. [Accessed: 03-Dec-2020].

[29] E. D. Weber and S. M. Borthwick, “Plasma Cortisol Stress Response of Juvenile Chinook Salmon to Passage through Archimedes Lifts and a Hidrostal Pump,” *North Am. J. Fish. Manag.*, vol. 22, pp. 563–570, 2002.

[30] M. G. Mesa, L. P. Gee, L. K. Weiland, and H. E. Christiansen, “Physiological Responses of Adult Rainbow Trout Experimentally Released through a Unique Fish Conveyance Device,” *North Am. J. Fish. Manag.*, vol. 33, pp. 1179–1183, 2013.

[31] A. Strizhak, U. Vakhidov, A. Lipin, R. Dorofeev, A. V Sogin, and L. S. Mazunova, “Modelling of vehicles with rotary-screw propulsion unit along water- flooded substructure Modelling of vehicles with rotary-screw propulsion unit along water-flooded substructure,” in *Journal of Physics: Conference Series*, 2019.

[32] M. DiFrangia, “The hydraulics of injection molders,” *FluidPower World*, Cleveland, May-2016.

[33] I. Bobbink, “De Landschapsarchitectuur van het Polder-boezemsysteem,” Sirene Ontwerpers, Rotterdam, 2016.

[34] L. B. Kreuziger and M. P. Massicotte, “Adult and pediatric mechanical circulation : a guide for the hematologist,” *Hematology*, vol. 2018, no. 1, pp. 507–515, 2018.

[35] S. R. Waters and G. A. Aggidis, “Over 2000 years in review: Revival of the Archimedes Screw from Pump to Turbine,” *Renew. Sustain. Energy Rev.*, vol. 51, pp. 497–505, 2015.

[36] W. Moerscher, “Water Power System,” US1434138A, 1922.

[37] K. Kawakami, “The Archimedes screw pump in Japan,” in *The 3rd International Conference on Business & Technology Transfer*, 2006, no. 3, pp. 29–33.

[38] A. Lashofer, “Projekt Wasserkraftschnecken Verortung,” *Ingenieurbüro Lashofer*, 2020. [Online].

706 Available: https://www.lashofer.at/deutsch/wasserkraftschnecke/projekt-wasserkraftschnecken-
707 verortung/. [Accessed: 05-May-2020].

708 [39] M. Shahsavarifard, A. H. Birjandi, E. L. Bibeau, and R. Sinclaire, “Performance characteristics of
709 the Energy Cat 3EC42 hydrokinetic turbine,” *MTS/IEEE Ocean. 2015 - Genova Discov. Sustain.*
710 *Ocean Energy a New World*, pp. 3–6, 2015.

711 [40] A. Stergiopoulou, V. Stergiopoulos, and E. Kalkani, “Experimental and theoretical research of zero
712 head innovative horizontal axis archimedean screw turbines,” *Int. J. Energy Environ.*, vol. 6, no. 5,
713 pp. 471–478, 2015.

714 [41] A. Lashofer, W. Hawle, and B. Pelikan, “State of technology and design guidelines for the
715 Archimedes screw turbine,” in *Hydro 2012 - Innovative Approaches to Global Challenges*, 2012,
716 no. October, pp. 1–8.

717 [42] A. Kozyn, S. Ash, and W. D. Lubitz, “Assessment of Archimedes Screw Power Generation Potential
718 in Ontario CCTC 2015 Paper Number 1570095585,” no. 1570095585, pp. 1–11, 2015.

719 [43] M. Lyons and W. D. Lubitz, “Archimedes screws for microhydro power generation,” in
720 *Proceedings of the ASME 2013 7th International Conference on Energy Sustainability & 11th Fuel*
721 *Cell Science*, 2013, pp. 1–7.

722 [44] J. Chen, H. X. Yang, C. P. Liu, C. H. Lau, and M. Lo, “A novel vertical axis water turbine for power
723 generation from water pipelines,” *Energy*, vol. 54, no. June 2013, pp. 184–193, 2013.

724 [45] J. Chen, W. Lu, Z. Hu, Y. Lei, and M. Yang, “Numerical studies on the performance of a drag-type
725 vertical axis water turbine for water pipeline,” *J. Renew. Sustain. Energy*, vol. 10, no. 4, 2018.

726 [46] A. Ghimire, D. R. Dahal, N. Pokharel, S. Chitrakar, B. S. Thapa, and B. Thapa, “Opportunities and
727 Challenges of introducing Francis Turbine in Nepalese Micro Hydropower Projects,” *J. Phys. Conf.*

Ser., vol. 1266, no. 1, 2019.

[47] M. M. Uamusse, M. Aljaradin, and K. M. Persson, “Micro-Hydropower Plant -Energy Solution Used in Rural Areas, Mozambique,” *Sustain. Resour. Manag. J.*, vol. 2, no. 1, pp. 3–9, 2017.

[48] C. S. Kaunda, C. Z. Kimambo, and T. K. Nielsen, “A technical discussion on microhydropower technology and its turbines,” *Renew. Sustain. Energy Rev.*, vol. 35, pp. 445–459, 2014.

[49] S. Sangal, A. Garg, and D. Kumar, “Review of Optimal Selection of Turbines for Hydroelectric Projects,” *Rev. Optim. Sel. Turbines Hydroelectr. Proj.*, vol. 3, no. 3, pp. 424–430, 2013.

[50] D. Matsushita, R. Moriyama, K. Nakashima, S. Watanabe, K. Okuma, and A. Furukawa, “Tentative study on performance of darriues-type hydroturbine operated in small open water channel,” *IOP Conf. Ser. Earth Environ. Sci.*, vol. 22, pp. 0–10, 2014.

[51] A. Kadier, M. S. Kalil, M. Pudukudy, H. A. Hasan, A. Mohamed, and A. A. Hamid, “Pico hydropower (PHP) development in Malaysia: Potential, present status, barriers and future perspectives,” *Renew. Sustain. Energy Rev.*, vol. 81, no. November 2017, pp. 2796–2805, 2018.

[52] E. McLean and D. Kearney, “An evaluation of seawater pumped hydro storage for regulating the export of renewable energy to the national grid,” *Energy Procedia*, vol. 46, pp. 152–160, 2014.

[53] R. Uhunmwangho, M. Odje, and K. E. Okedu, “Comparative analysis of mini hydro turbines for Bumaji Stream, Boki, Cross River State, Nigeria,” *Sustain. Energy Technol. Assessments*, vol. 27, no. June, pp. 102–108, 2018.

[54] R. Fraser, C. Deschênes, C. O’Neil, and M. Leclerc, “VLH: Development of a new turbine for Very Low Head sites,” *Proc. 15th Waterpower*, vol. 10, no. 157, pp. 1–9, 2007.

[55] P. Kemp, C. Williams, R. Sasseville, and N. Anderson, “Very low head turbine deployment in

Canada," *IOP Conf. Ser. Earth Environ. Sci.*, vol. 22, 2014.

[56] W. Nuantong and S. Taechajedcadarungsri, "Optimal design of VLH axial hydro-turbine using regression analysis and multi-objective function (GA) optimization methods," *J. Appl. Fluid Mech.*, vol. 9, no. 5, pp. 2291–2298, 2016.

[57] J. Razak, Y. Ali, and M. Alghoul, "Application of crossflow turbine in off-grid pico hydro renewable energy system," *Recent Adv. Appl. Math.*, no. January, pp. 519–526, 2010.

[58] A. K. Yahya, W. N. W. A. Munim, and Z. Othman, "Pico-hydro power generation using dual pelton turbines and single generator," *Proc. 2014 IEEE 8th Int. Power Eng. Optim. Conf. PEOCO 2014*, no. March, pp. 579–584, 2014.

[59] E. Quaranta, "Stream water wheels as renewable energy supply in flowing water: Theoretical considerations, performance assessment and design recommendations," *Energy Sustain. Dev.*, vol. 45, pp. 96–109, 2018.

[60] E. Quaranta, "Estimation of the permanent weight load of water wheels for civil engineering and hydropower applications and dataset collection," *Sustain. Energy Technol. Assessments*, vol. 40, no. June, pp. 1–8, 2020.

[61] E. Quaranta and R. Revelli, "Gravity water wheels as a micro hydropower energy source: A review based on historic data, design methods, efficiencies and modern optimizations," *Renew. Sustain. Energy Rev.*, vol. 97, no. November 2017, pp. 414–427, 2018.

[62] MJ2 Technologies S.A.S., "Case Studies: VLH Turbines," *Sorgent.e Capital*, 2018. [Online]. Available: www.vlh-turbine.com/documents/%0D. [Accessed: 12-Jul-2020].

[63] I. Hydropower Turbine Systems, "Ossberger Hydro Projects," *ossbergerhydro.com*, 2019. [Online]. Available: http://www.ossbergerhydro.com/projects.html. [Accessed: 14-Jul-2020].

[64] Voith GmbH & Co. KGaA, “Kaplan turbines,” *voith.com*, 2018. [Online]. Available: http://www.voith.com/ca-en/products-services/hydro-power/turbines/kaplan-turbines-560.html. [Accessed: 14-Jul-2020].

[65] GE Renewable Energy Division, “Kaplan hydro turbine,” *ge.com*, 2019. [Online]. Available: https://www.ge.com/renewableenergy/hydro-power/large-hydropower-solutions/hydro-turbines/kaplan-turbine. [Accessed: 15-Jul-2020].

[66] M. Eisenring, *Micro Pelton Turbines*, 1st ed. St. Gallen, Switzerland: Swiss Center for Appropriate Technology, 1991.

[67] Gruner AG, “Akköy ll: Giresun, Turkey,” *gruner.ch*, 2019. [Online]. Available: https://www.gruner.ch/en/references/styt-ref-d-akkoey-ll. [Accessed: 16-Jul-2020].

[68] Gilbert Gilkes & Gordon Ltd., “Case Studies: Our global projects,” *gilkes.com*, 2020. [Online]. Available: https://www.gilkes.com/case-studies. [Accessed: 15-Jul-2020].

[69] N. Bard, “River Dart Hydro Performance Assessment By Nick Bard Hydro Services For Mannpower Consulting Ltd,” *Nick Bard Hydro Serv.*, vol. 44, no. 0, 2007.

[70] A. Kozyn and W. D. Lubitz, “A power loss model for Archimedes screw generators,” *Renew. Energy*, vol. 108, pp. 260–273, 2017.

[71] N. Fergnani and P. Silva, “Technical and economic assessment of an Archimedean screw with variable speed operation under variable flows,” Milan, 2016.

[72] Landustrie Sneek BV, “Hydropower: Windsor Castle (UK),” *Landustrie.nl*, 2019. [Online]. Available: https://www.landustrie.nl/en/products/hydropower/projects/windsor.html. [Accessed: 25-Sep-2019].

[73] Landustrie Sneek BV, “Hydropower: Linton Lock (UK),” *Landustrie.nl*, 2017. [Online]. Available: https://www.landustrie.nl/en/products/hydropower/projects/linton-lock.html. [Accessed: 03-Mar-2020].

[74] Landustrie Sneek BV, “Large hydropower scheme in Alsace,” *Landustrie.nl*, 2016. [Online]. Available: https://www.landustrie.nl/en/news/news/archive/2016/11/article/large-hydropower-scheme-in-alsace-107.html. [Accessed: 16-Apr-2020].

[75] C. M. Pringle, M. C. Freeman, and B. J. Freeman, “Regional Effects of Hydrologic Alterations on Riverine Macrobiota in the New World,” *Bioscience*, vol. 50, no. 9, pp. 807–823, 2000.

[76] R. J. Neves, A. E. Bogan, J. D. Williams, S. A. Ahlstedt, and P. W. Hartfield, “Status Of Aquatic Mollusks in the southeastern United States: a downward spiral of diversity,” in *Aquatic fauna in peril: the southeastern perspective*, 1st ed., Decatur: Southeast Aquatic Research Institute Special Publication, 1997, pp. 43–85.

[77] P. McCully, *Silenced rivers: The ecology and polititcs of large dams*. London: Zed Books, 1996.

[78] L. Yang, F. Lu, X. Zhou, X. Wang, X. Duan, and B. Sun, “Progress in the studies on the greenhouse gas emissions from reservoirs,” *Acta Ecol. Sin.*, vol. 34, no. 4, pp. 204–212, 2014.

[79] B. R. Deemer *et al.*, “Greenhouse gas emissions from reservoir water surfaces: A new global synthesis,” *Bioscience*, vol. 66, no. 11, pp. 949–964, 2016.

[80] P. Fearnside, “Greenhouse Gas Emissions from a Hydroelectric Reservoir (Brazil’s Tucurui Dam) and the Energy Policy Impactions,” *Water Air Soil Pollut.*, 2002.

[81] D. Kasper *et al.*, “Reservoir stratification affects methylmercury levels in river water, plankton, and fish downstream from Balbina hydroelectric dam, Amazonas, Brazil,” *Environ. Sci. Technol.*, vol. 48, no. 2, pp. 1032–1040, 2014.

[82] W. Wildi, “Environmental hazards of dams and reservoirs,” *NEAR Curric. Nat. Environ. Sci.*, vol. 88, pp. 187–197, 2010.

[83] N. G. Miles and R. J. West, “The use of an aeration system to prevent thermal stratification of a freshwater impoundment and its effect on downstream fish assemblages,” *J. Fish Biol.*, vol. 78, no. 3, pp. 945–952, 2011.

[84] A. R. Abernathy and P. M. Cumbie, “Mercury accumulation by largemouth bass (Micropterus salmoids) in recently impounded reservoirs,” *Bull. Environ. Contam. Toxicol.*, vol. 17, no. 5, 1977.

[85] R. S. D. Calder, A. T. Schartup, M. Li, A. P. Valberg, P. H. Balcom, and E. M. Sunderland, “Future Impacts of Hydroelectric Power Development on Methylmercury Exposures of Canadian Indigenous Communities,” *Environ. Sci. Technol.*, p. acs.est.6b04447, 2016.

[86] D. Kumar and S. S. Katoch, “Environmental sustainability of run of the river hydropower projects: A study from western Himalayan region of India,” *Renew. Energy*, vol. 93, pp. 599–607, 2016.

[87] C. D. McNabb, C. R. Liston, and S. M. Borthwick, “Passage of Juvenile Chinook Salmon and other Fish Species through Archimedes Lifts and a Hidrostal Pump at Red Bluff, California,” *Trans. Am. Fish. Soc.*, vol. 132, no. 1985, pp. 326–334, 2003.

[88] C. Wolter, D. Bernotat, J. Gessner, A. Brüning, J. Lackemann, and J. Radinger, “Fachplanerische Bewertung der Mortalität von Fischen an Wasserkraftanlagen,” Bonn, 2020.

[89] C. A. Boys, B. D. Pfugrath, M. Mueller, J. Pander, Z. D. Deng, and J. Geist, “Physical and hydraulic forces experienced by fish passing through three different low-head hydropower turbines,” *Mar. Freshw. Res.*, no. 69, pp. 1934–1944, 2018.

[90] I. S. Pauwels *et al.*, “Multi-Species Assessment of Injury , Mortality , and Physical Conditions during Downstream Passage through a Large Archimedes Hydrodynamic Screw,” *Sustainability*,

836 vol. 12, no. 8722, pp. 1–25, 2020.

837 [91] P. Kibel and T. Coe, “Fish Monitoring and Live Fish Trials. Archimedes Screw Turbine, River Dart.,”
838 Moretonhampstead, Devon, 2007.

839 [92] A. T. Piper, P. J. Rosewarne, R. M. Wright, and P. S. Kemp, “The impact of an Archimedes screw
840 hydropower turbine on fi sh migration in a lowland river,” *Ecol. Eng.*, vol. 118, no. March 2018,
841 pp. 31–42, 2018.

842 [93] P. Kibel, “Archimedes Screw Turbine Fisheries Assessment. Phase II: Eels and Kelts,”
843 Moretonhampstead, Devon, 2008.

844 [94] C. Elliott, “Personal Communication with Chris Elliott.” Fishtek Consulting, Totnes, England, 2019.

845 [95] United Kingdom Environment Agency, “Hydropower Good Practice Guidelines Screening
846 requirements,” York, England, 2012.

847 [96] T. B. Havn *et al.*, “Downstream migration of Atlantic salmon smolts past a low head hydropower
848 station equippped with Archimedes screw and Francis turbines,” *Ecol. Eng.*, vol. 105, pp. 262–
849 275, 2017.

850 [97] D. Bennion, “Maintaining Archimedes Screw Pumps,” *ECS Engineering Services*, 2013. [Online].
851 Available: http://www.ecsengineeringservices.com/maintaining-archimedes-screw-pumps/.
852 [Accessed: 10-Oct-2019].

853 [98] D. Dechambeau, “Personal Communication with David Dechambeau.” Southeast Power
854 Engineering Ltd, Windsor, England, 2019.

855 [99] Spaans Babcock Hydro Power, “Archimedean Screw Turbine.” Spaans Babcock Hydro Power,
856 Balk, 2012.

[100] D. Nuernbergk, *Wasserkraftschnecken - Berechnung und optimaler Entwurf von archimedischen Schnecken als Wasserkraftmaschine (Hydropower screws - Calculation and Design of Archimedes Screws used in Hydropower)*, 1st ed. Detmold: Verlag Moritz Schäfer, 2012.

[101] S. Simmons, K. Songin, and W. Lubitz, "Experimental investigation of the factors affecting Archimedes screw generator power output," in *HYDRO 2017 (7-11 October 2017)*, 2017.

[102] K. Songin, "Experimental Analysis of Archimedes Screw Turbines," University of Guelph, 2017.

[103] G. Dellinger, S. Simmons, W. D. Lubitz, P. A. Garambois, and N. Dellinger, "Effect of slope and number of blades on Archimedes screw generator power output," *Renew. Energy*, no. June, pp. 896–908, 2019.

[104] W. D. Lubitz, M. Lyons, and S. Simmons, "Performance Model of Archimedes Screw Hydro Turbines with Variable Fill Level," *J. Hydraul. Eng.*, vol. 140, no. 10, pp. 1–11, 2014.

[105] D. M. Nuernbergk, *Wasserkraftschnecken - Berechnung und optimaler Entwurf von archimedischen Schnecken als Wasserkraftmaschine (Hydropower screws - Calculation and Design of Archimedes Screws used in Hydropower)*, 2nd ed. Detmold: Verlag Moritz Schäfer, 2020.

[106] N. Fergnani, "Personal Communication with Nicola Fergnani." HydroSmart Srl, Ferrara, Italy, 2019.

[107] G. Nagel, *Archimedian Screw Pump Handbook: Fundamental Aspects of the Design and Operation of Water Pumping Installations Using Archimedian Screw Pumps*, 1st ed. Schwäbisch Gmünd: RITZ-Pumpenfabrik OHG, 1968.

[108] M. Lisicki, W. Lubitz, and G. W. Taylor, "Optimal design and operation of Archimedes screw turbines using Bayesian optimization," *Appl. Energy*, vol. 183, pp. 1404–1417, 2016.

[109] C. Elliott, *Planning and Installing Micro-Hydro Systems: A Guide for Designers, Installers and Engineers*. Abingdon: Routledge, 2014.

[110] J. Muysken, “Berekening van het nuttig effect van de vijzel,” *Ing.*, vol. 21, pp. 77–91, 1932.

[111] M. Lyons, “Lab Testing and Modeling of Archimedes Screw Turbines,” University of Guelph, 2014.

[112] D. Mann, “Mann Power installs turbine at birthplace of hydropower,” *mannpower-hydo.co.uk*, 2015. [Online]. Available: http://www.mannpower-hydro.co.uk/1731-2/. [Accessed: 18-Dec-2019].

[113] S. Simmons, M. Lyons, G. Dellinger, and W. Lubitz, “Effects of varying inclination angle on Archimedes screw generator power production with constant head,” in *Proceedings of The Joint Canadian Society for Mechanical Engineering and CFD Society of Canada International Congress 2019*, 2019.

[114] Erinofiardi *et al.*, “Experimental Study of Screw Turbine Performance based on Different Angle of Inclination,” in *Energy Procedia*, 2017, vol. 110, no. December 2016, pp. 8–13.

[115] K. Brada, “Wasserkraftschnecke ermöglicht Stromerzeugung über Kleinkraftwerke [Hydraulic screw generates electricity from micro hydropower stations],” *Maschinenmarkt Würzbg.*, no. 14, pp. 52–56, 1999.

[116] A. Lashofer, W. Hawle, F. Kaltenberger, and B. Pelikan, “Die Wasserkraftschnecke – Praxis, Prüfstand und Potenzial,” *Österreichische Wasser- und Abfallwirtschaft*, vol. 65, no. 9–10, pp. 339–347, 2013.

[117] A. Kozyn and W. Lubitz, “Experimental Validation of Gap Leakage Flow Models in Archimedes Screw Generators,” in *Renewable Energy in the Service of Mankind Vol I*, Sayigh A., Ed. Cham: Springer International Publishing Switzerland, 2015, pp. 365–375.

[118] K. J. Songin and W. D. Lubitz, “Measurement of fill level and effects of overflow in power-generating Archimedes screws,” *J. Hydraul. Res.*, vol. 57, no. 5, pp. 635–646, 2018.

[119] A. Passamonti, “Investigation of energy losses in laboratory and full-scale Archimedes screw generators,” Politechnico di Milano, 2017.

[120] G. Dellinger, S. Simmons, W. D. Lubitz, P.-A. Garambois, and N. Dellinger, “Effect of slope and number of blades on Archimedes screw generator power output,” *Renew. Energy*, no. Online January 2019, 2018.

[121] A. Khan, S. Simmons, M. Lyons, and W. Lubitz, “Inlet Channel Effects on Archimedes Screw Generators,” in *Proceedings of The Canadian Society for Mechanical Engineering International Congress 2018*, 2018.

[122] M. Lyons, S. Simmons, M. Fisher, J. S. Williams, and W. D. Lubitz, “Experimental Investigation of Archimedes Screw Pump,” *J. Hydraul. Eng.*, vol. 146, no. 8, pp. 1–10, 2020.

[123] J. Rohmer, D. Knittel, G. Sturtzer, D. Flieller, and J. Renaud, “Modeling and experimental results of an Archimedes screw turbine,” *Renew. Energy*, vol. 94, pp. 136–146, 2016.

[124] G. Dellinger, A. Terfous, P.-A. Garambois, and A. Ghenaim, “Experimental investigation and performance analysis of Archimedes screw generator,” *J. Hydraul. Res.*, vol. 1686, no. April, 2016.

[125] G. Dellinger *et al.*, “Computational fluid dynamics modeling for the design of Archimedes Screw Generator,” *Renew. Energy*, vol. 118, pp. 847–857, 2018.

[126] T. Saroinsong, R. Soenoko, S. Wahyudi, and M. N. Sasongko, “The effect of head inflow and turbine axis angle towards the three row bladed screw turbine efficiency,” *Int. J. Appl. Eng. Res.*, vol. 10, no. 7, pp. 16977–16984, 2015.

[127] A. I. Siswantara, Warjito, Budiarso, R. Harmadi, M. H. Gumelar, and D. Adanta, “Investigation of the α angle’s effect on the performance of an Archimedes turbine,” *Energy Procedia*, vol. 156, pp. 458–462, 2019.

[128] T. Saroinsong, R. Soenoko, S. Wahyudi, and M. N. Sasongko, “Fluid Flow Phenomenon in a Three-Bladed Power-Generating Archimedes Screw Turbine,” *J. Eng. Sci. Technol. Rev.*, vol. 9, no. 2, pp. 72–79, 2016.

[129] K. Anzawa, A. Müller, T. Tanaka, and K. Yamaishi, “Small Hydro from Fukushima – An Energy Revolution 1 kW at a Time,” in *HydroVision 2017*, 2017, no. July.

[130] M. Johnson and M. Jensen, “A New Twist on Archimedes’ Screw.” Utah State University - College of Engineering, Logan, Utah, pp. 1–2, 2018.

[131] A. Kozyn, K. Songin, B. Gharabaghi, and W. D. Lubitz, “Predicting Archimedes Screw Generator Power Output Using Artificial Neural Networks,” *J. Hydraul. Eng.*, vol. 144, no. 3, pp. 1–8, 2018.

[132] N. Fergnani, P. Silva, and D. Bavera, “Efficiency assessment of a commercial size Archimedean screw turbine based on experimental data,” in *Hydro 2017*, 2017.

[133] R. Dhakal *et al.*, “Prospects of off Grid Energy Generation through Low Head Screw Turbine in Nepal,” *7th Int. IEEE Conf. Renew. Energy Res. Appl. ICRERA 2018*, no. December, pp. 537–543, 2018.

[134] T. Okamura, R. Kurosaki, and M. Takano, “Development and Introduction of a Pico-Hydro System in Southern Tanzania,” *Afr. Study Monogr.*, vol. 36, no. 2, pp. 117–137, 2015.

[135] J. Kleemann and D. H. Hellmann, “Gutachten zur Wirkungsgradbestimmung an einer Wasserkraftschnecke Fabrikat RITZ-ATRO,” Kaiserslautern, 2003.

943 [136] N. Fergnani and P. Silva, “Archimedean screw and intake head losses : design optimization under
944 variable flows and variable speed,” in *Hydro 2016*, 2016.

945 [137] N. Fergnani and P. Silva, “Energetic and economic assessment of an Archimedean screw with
946 variable speed operation under variable flows,” in *HYDRO 2015*, 2015.

947 [138] K. Shahverdi *et al.*, “Energy harvesting using solar ORC system and Archimedes Screw Turbine
948 (AST) combination with different refrigerant working fluids,” *Energy Convers. Manag.*, vol. 187,
949 no. October 2018, pp. 205–220, 2019.

950 [139] G. Müller and J. Senior, “Simplified theory of Archimedean screws,” *J. Hydraul. Res.*, vol. 47, no.
951 5, pp. 666–669, 2009.

952 [140] D. M. Nuernbergk and C. Rorres, “An Analytical Model for the Water Inflow of an Archimedes
953 Screw Used in Hydropower Generation,” *J. Hydraul. Eng.*, vol. 139, no. 2, p. 120723125453009,
954 2012.

955 [141] N. Johnson, J. Kang, S. Sharples, A. Hathway, and P. Dökmeci, “Acoustic Impact of An Urban Micro
956 Hydro Scheme,” *Proc. World Renew. Energy Congr. – Sweden, 8–13 May, 2011, Linköping,*
957 *Sweden*, vol. 57, pp. 1448–1455, 2011.

958 [142] A. Clayton, “Personal Communication with Adrian Clayton.” Mannpower, York, England, 2019.

959 [143] D. Mann, “Personal Communiation with David Mann.” Mannpower, York, England, 2019.

960 [144] W. D. Lubitz, “Gap Flow in Archimedes Screws,” *CSME Int. Congr. 2014*, no. June, pp. 1–6, 2014.

961 [145] S. Simmons, “A Computational Fluid Dynamic Analysis of Archimedes Screw Generators,”
962 University of Guelph, 2018.

963 [146] S. C. Simmons and W. D. Lubitz, “Analysis of internal fluid motion in an Archimedes screw using

computational fluid mechanics," *J. Hydraul. Res.*, 2020.

[147] D. Aigner, "Überfälle," in *Wasserbauliche Mittelungen – Aktuelle Forschungen im Wasserbau 1993 - 2008*, H. B. Horlacher and K.-U. Graw, Eds. Dresden: Technischen Universität Dresden, 2008, pp. 182–200.

[148] S. Simmons, G. Dellinger, M. Lyons, A. Terfous, A. Ghenaim, and W. D. Lubitz, "The effects of inclination angle on Archimedes screw generator power production with constant head," *J. Hydraul. Res.*, 2020.

[149] G. Dellinger, P. Garambois, M. Dufresne, A. Terfous, J. Vazquez, and A. Ghenaim, "Numerical and experimental study of an Archimedean Screw Generator," *28th AHR Symp. Hydraul. Mach. Syst. Grenoble, July 4-8*, vol. 2, pp. 1419–1428, 2016.

[150] M. I. Maulana, A. Syuhada, and F. Almas, "Computational fluid dynamic predictions on effects of screw number on performance of single blade Archimedes screw turbine," in *E3S Web of Conferences*, 2018, vol. 67.

[151] M. Shimomura and M. Takano, "Modeling and Performance Analysis of Archimedes Screw Hydro Turbine Using Moving Particle Semi-Implicit Method," *J. Comput. Sci. Technol.*, vol. 7, no. 2, pp. 338–353, 2013.

[152] M. Haselbauer and F. E. Hammerl, "Reducing Noise in Hydrodynamic Screws," *Flow Science, Inc.*, 2012. [Online]. Available: https://www.flow3d.com/hydrodynamic-screws/. [Accessed: 08-May-2020].

[153] A. Stergiopoulou, V. Stergiopoulos, and E. Kalkani, "Computational Fluid Dynamics study on a 3D graphic solid model of archimedean screw turbines," *Int. Conf. Environ. Manag. Eng. Planning, Econ.*, vol. 23, no. 11, pp. 7–14, 2014.

[154] J. Adlard, “Archimedes’ screw: Copley Hydropower Generator,” Future Energy Yorkshire, Yorkshire, 2011.

[155] O. M. Dada, I. A. Daniyan, and O. . Adaranola, “Optimal Design of Micro Hydro Turbine (Archimedes Screw Turbine) in Arinta Waterfall in Ekiti State, Nigeria,” vol. 4, no. 2, pp. 34–38, 2014.

[156] Renewables First, “How much does a hydropower system cost to operate?,” *renewablesfirst.co.uk*, 2015. [Online]. Available: https://www.renewablesfirst.co.uk/hydropower/hydropower-learning-centre/how-much-does-a-hydropower-system-cost-to-operate/. [Accessed: 11-May-2020].

[157] Renewables First, “How much does a hydropower system cost to build?,” *renewablesfirst.co.uk*, 2015. [Online]. Available: https://www.renewablesfirst.co.uk/hydropower/hydropower-learning-centre/how-much-do-hydropower-systems-cost-to-build/. [Accessed: 11-May-2020].

[158] M. Harris, “260 kW Archimedes Screw hydropower plant begins operation near Kilnhurst,” *Hydro Review*, Kilnhurst, 16-Oct-2015.

[159] P. Parker and M. Moreno, “A feasibility study into the use of an Archemidian screw turbine for hydroelectric generation at Teddington Weir, London,” London, 2009.

[160] Esk Energy (Yorkshire) Ltd., “The Whitby Esk Energy - Ruswarp Hydro,” *whitbyeskenergy.org.uk*, 2020. [Online]. Available: https://whitbyeskenergy.org.uk/. [Accessed: 05-May-2020].

[161] Torrs Hydro New Mills Ltd., “Torrs Hydro: The Project,” *torrshydro.org*, 2020. [Online]. Available: http://www.torrshydro.org/. [Accessed: 05-May-2020].

[162] S. Simmons, G. Dellinger, M. Lyons, A. Terfous, A. Ghenaim, and W. D. Lubitz, “Effects of Inclination Angle on Archimedes Screw Generator Power Production with Constant Head,” *J.*

Hydraul. Eng., vol. 147, no. 3, pp. 1–12, 2021.

Appendix

Table A1: Index of example hydropower plants from Fig. 2. Turbine types are identified as follows: Archimedes screw generators (A), Crossflow turbines (C), Kaplan/Propeller type turbines (K), Francis turbines (F), Pelton turbines (P), Turgo turbines (T), VLH turbines (V), Undershot waterwheels (U), Overshot waterwheels (O), and Breast-shot waterwheels (B). Data from various sources [44], [45], [54]–[63], [46], [64]–[68], [47]–[53]**.**

Site Number	Turbine Type	Site Identification	City	Country	Q (m^3/s)	H (m)	Reference
1	A	Widdington	Linton-on-Ouse	UK	14.5	3	https://www.landustrie.nl/
2	A	PicoPica	Ena	Japan	0.01	0.1	http://www.unido.or.jp/en/technology_db/5276/
3	A	Buckfast Abbey	Buckfastleigh	UK	2.33	4.33	https://www.renewablesfirst.co.uk/
4	C	Universiti Kebangsaan Malaysia	Bangi	Malaysia	0.02	1.2	Razak et al. (2010)
5	C	Elora	Elora	Canada	8.8	11.6	http://www.ossbergerhydro.com/projects.html
6	C	Aspen	Aspen	Colorado	1	47.5	http://www.ossbergerhydro.com/projects.html
7	K	Novarina	-	-	0.58	4.85	Quaranta (2020)
8	K	Engineer Sérgio Motta Dam	São Paulo	Brazil	950	10	https://www.ge.com/renewableenergy/
9	K	Peixe Angical	Peixe	Brazil	293.3	40.9	http://voith.com/
10	F	HS Dynamic	Hong Kong	China	0.05	12	https://www.hs-dynamics.com/
11	F	Candelaria	Chisec	Guatemala	3.79	129.45	https://www.gilkes.com/
12	F	Jhimuk Hydropower Plant	Khaira	Nepal	513.9	162	https://nwrmap.info/hydropower/
13	P	Blair Castle	Blair Atholl	UK	0.092	112	https://www.gilkes.com/
14	P	La Esmeralda Dam	Chivor	Columbia	20	800	https://www.hydropower.org/case-studies/
15	P	Hidroelectrica Choloma S.A	Guatemala City	Guatemala	2.5	438	https://www.gilkes.com/
16	T	Balbeg	Inverness	UK	0.15	30	http://www.highlandeco.com/
17	T	Grytviken	Grytviken	South Georgia	0.472	65	https://www.gilkes.com/
18	T	Pungwe B	Honde Valley	Zimbawe	3	176	https://www.gilkes.com/
19	V	Isola Dovarese HPP	Isola Dovarese	Italy	11.75	3.2	http://www.vlh-turbine.com/
20	U	Queen's Mill	Castelford	UK	3.9	2.1	Quaranta (2020)
21	U	Undershot Waterwheel	-	-	0.28	0.58	Quaranta (2020)
22	U	Treviso Waterwheel	Treviso	Italy	1.38	0.95	Quaranta (2020)
23	O	Hydrowatt	-	-	0.6	3	Quaranta and Revelli (2018)
24	O	Cooperation project MAE-FAO	-	Italy	0.04	5.5	Quaranta and Revelli (2018)
25	O	Alan Stoyel and Graham Hackney	-	-	0.15	3.5	Quaranta (2020)
26	B	Moter Saenger	-	-	0.7	2.6	Quaranta (2020)
27	B	Rigamonti Giovanni	Pusiano	Italy	0.1	1.6	Quaranta (2020)
28	B	The Mill of Borgo Cornalese	Villastellone	Italy	1	1.85	Quaranta and Revelli (2018)